Strojniški vestnik - Journal of Mechanical Engineering 53(2007)3, 165-172
UDK - UDC [620.179.13:620.193]:519.876.5
Kratki znanstveni prispevek - Short scientific paper (1.03)

Numerični pristop toplotnih neporušnih preiskav skritih okvar

A Numerical Approach to Hidden Defects in Thermal Non-Destructive Testing

Srećko Švaić - Ivanka Boras - Mladen Andrassy
(University of Zagreb, Croatia)

Uporaba infrardeče (IR) termografije kot neškodljiva preizkusna metoda za odkrivanje napak pod površino ter tudi za določevanje jakosti korozije veliko obeta. Razen omejitev, ki so posledica IR kamere same in toplotnih lastnosti preizkušanega materiala, nam da IR termografija v povezavi z ustrezno numerično metodo sprejemljive rezultate. Numerično simuliranje prenosa toplote nam omogoči ločeno analizo primernih parametrov, ki določijo razširjanje toplote v materialu, kot so: jakost in trajanje toplotnega vzbujanja, lastnosti materiala in začetni pogoji, prav tako pa tudi časovno porazdelitev nekaterih parametrov. Primerjava numerične simulacije in termografskih meritev, opisanih v [5], je dala zelo dobro ujemanje rezultatov. Iz numerične analize je jasno razvidna pomembnost določitve trenutka, ko kontrast doseže svojo največjo vrednost. Analiza nam prav tako pokaže, da lahko relativno izgubo materiala in premer napake določimo z največjo točnostjo v trenutku, ko kontrast doseže svojo največjo vrednost.

(Ključne besede: neporušno preizkušanje, termografija, metode nadzornih prostornin, numerično simuliranje)

The application of infrared (IR) thermography for detecting defects under the surface as well as for the estimation of the corrosion intensity seems to have good prospects as a non-destructive testing method. Besides the limitations which are the result of the IR camera itself and the thermal properties of the material detected, IR thermography produces acceptable results when combined with an appropriate numerical method. A numerical simulation of heat transport makes possible a separate analysis of the relevant parameters that characterize heat dissipation in the material, like the intensity and duration of the heat stimulation, the properties of the material and the starting conditions, as well as the time distribution of certain parameters. The comparison of a numerical simulation and thermographic measurements presented in [5] shows a very good agreement of the results. The importance of determining the moment when the contrast reaches its maximum can be clearly seen from the numerical analysis. The analysis also shows that a relative material loss and the diameter of the defect can be estimated with the best accuracy at the moment when the current contrast reaches its maximum.

(Keywords: non-destructive testing, thermography, control volume methods, numerical simulations)

0 INTRODUCTION

The development of thermal non-destructive testing (TNDT) started with the introduction of the first infrared sensors. Basically, the method consists of the thermal treatment of a sample and of the measuring of its thermal response in the spatial and temporal domain, $\vartheta=\vartheta(x,y,z,t)$. Experimentally, the method is based on recording the temperature distribution of a reference sample surface over time, using one of the known methods of infrared (IR) radiation recording. The theoretical part is reduced to solving the problem of heat conduction through the sample in the 1D, 2D or 3D domain over time.

The temperature field at the sample surface is the basis of all further analyses and conclusions on the possible presence of defects under the material surface and their parameters. The detection of a

defect expressed by the discontinuity of the temperature field at the sample surface depends on the changes of thermodynamic and physical properties of the sample.

With regard to the temperature field, it is necessary to take into account all the additional influences important in forming the object temperature image (anisotropy of the basic sample material, variations in the surface state and the object's thermal stimulation, noise from measuring equipment, etc.), and to distinguish between a real defect and the artefact.

The paper presents the results of an examination of two models: one with defects underneath its surface made from a different material and the other with corrosion defects. The numerical simulation performed for both models is in fair accordance with measurement results.

1 THE BASICS OF THERMAL NON-DESTRUCTIVE TESTING

Although the beginning of thermal non-destructive testing is attributed to the time when the first IR detectors were discovered in 1914, and almost all TNDT methods used today were developed from the 1960s until the end of the 1970s, these methods did not yield the results expected in comparison with other non-destructive testing (NDT) methods. A major change occurred when a thermodynamic approach to the problem of heat conduction and transfer was introduced into the measurement result analysis. Basically, the method may be reduced to a number of steps: thermal stimulation of the object, surface temperature recording (temperature response), data processing and decision making.

The choice of the object thermal stimulation depends on the type of control to be performed (final testing, corrosion detection, improvement of visibility of impurities in the basic material, etc.). Rapid heating or cooling of the sample leads to the sudden appearance of hot or cold areas at the sample surface, and a high sensitivity of measurement may be achieved. Heating or cooling may be applied to the front or the rear side of the sample, depending on the purpose of the procedure. The front or the rear sample side refers to the surface to be inspected.

Nowadays TNDT methods are divided into two basic groups: methods for preventive maintenance and methods developed for special needs of defect detection in the material [1].

The choice of a TNDT method depends on the type of defect expected underneath the material surface, the object accessibility from both sides and geometrical characteristics of the sample.

The basic defect types in the object are as follows: surface or inside cracks, impurities in the material, surface roughness, variations of the coating thickness, poor clinging of the coating, surface delaminates and corrosion. The thermal properties of a solid may be regarded as functions of spatial coordinates $\lambda = \lambda(x,y,z)$ and $a = a(x,y,z)$. Every interruption or steep change of these functions represents a potential defect (impurity) in the basic material. The analysis of the functions $\lambda(x,y,z)$ and $a = a(x,y,z)$ represents the material analysis of the sample.

The problems TNDT deals with include temperature functions depending on numerous parameters, such as spatial coordinates, time, dimensions of the sample and its thermal properties, defect dimensions and thermal properties, and heat-exchange parameters. All these parameters have to be taken into account when evaluating measurement results and defining the defect parameters, e.g., position, shape, dimensions and thermal properties.

The basic parameter in TNDT analysis is a quantity defined as the contrast. There are several definitions of contrast [1]:

a) Temperature contrast, defined as the difference of the temperatures of spots at the object representing a sound material and a material with impurities:

$$\Delta T(t) = T_{nd}(x,y,t) - T_d(x,y,t) \qquad (1).$$

b) Instantaneous (current) contrast, defined as the ratio of the temperature contrast and the sound material temperature:

$$C_r = \frac{T_{nd}(x,y,t) - T_d(x,y,t)}{T_{nd}(x,y,t)} = 1 - \frac{T_d(x,y,t)}{T_{nd}(x,y,t)} \qquad (2).$$

c) Normalized contrast defined as a difference of ratia:

$$C_n = \frac{T_d(x,y,t)}{T_d^{\,m}(x,y,t)} - \frac{T_{nd}(x,y,t)}{T_{nd}^{\,m}(x,y,t)} \qquad (3),$$

where the quantities in the denominators represent the peak temperatures at the chosen object surface spots with and without defects.

The selection of the contrast calculation mode during the analysis of the results also brings

along possible dependences of the chosen contrast type on the process parameters, the heat flux density in the first place, sample heating time, uniformity of the thermal stimulation, as well as the uniformity of the optical properties of the object surface, the distance between the spots of the object surface, the temperatures that are taken for the contrast calculation and other parameters.

In order to achieve a simpler result analysis and to enable a comparison with other investigations, one should apply the contrast types that are less dependent on the process parameters and more dependent on the state of the material underneath the object surface as more appropriate.

2 NUMERICAL METHODS IN THERMAL NON-DESTRUCTIVE TESTING

A numerical simulation of heat transport through an object with defects makes it possible to evaluate the behaviour of various types of defects (position, geometry, defect material properties) with different initial and boundary conditions, without the noise that is normally present in experiments. A comparison of the results of the numerical analysis performed using the control volume method with the measurement results confirms the reliability of the numerical procedure.

The procedure of the numerical analysis of heat transport starts with the three-dimensional non-steady heat-transport equation in rectangular coordinates:

$$\rho\, c\frac{\partial \vartheta}{\partial t}=\frac{\partial}{\partial x}\left(\lambda\frac{\partial \vartheta}{\partial x}\right)+\frac{\partial}{\partial y}\left(\lambda\frac{\partial \vartheta}{\partial y}\right)+\frac{\partial}{\partial z}\left(\lambda\frac{\partial \vartheta}{\partial z}\right)+\phi_v \quad (4),$$

where: ρ – density, kg/m^3

c – specific heat capacity, J/(kgK)

λ – thermal conductivity, W/(mK)

ϑ – temperature, °C

x, y, z – spatial coordinates, m

ϕ – heat source or sink, W/m^3

Equation (5) is obtained by implicitly discretizing equation (4) [2]:

$$a_P\,\vartheta_P = a_E\,\vartheta_E + a_W\,\vartheta_W + a_N\,\vartheta_N + \\ + a_S\,\vartheta_S + a_T\,\vartheta_T + a_B\,\vartheta_B + b \quad (5),$$

with coefficients:

$$a_E=\lambda_e\frac{\Delta y\cdot\Delta z}{(\delta_x)_e} \qquad a_W=\lambda_w\frac{\Delta y\cdot\Delta z}{(\delta_x)_w}$$

$$a_N=\lambda_n\frac{\Delta x\cdot\Delta z}{(\delta_y)_n} \qquad a_S=\lambda_s\frac{\Delta x\cdot\Delta z}{(\delta_y)_s}$$

$$a_T=\lambda_t\frac{\Delta x\cdot\Delta y}{(\delta_z)_t} \qquad a_B=\lambda_b\frac{\Delta x\cdot\Delta y}{(\delta_z)_b}$$

$$b=\phi_v\cdot\Delta x\cdot\Delta y\cdot\Delta z+a_P^o\cdot\vartheta_P^o \quad (7)$$

$$a_P^o=\frac{\rho\cdot c\cdot\Delta x\cdot\Delta y\cdot\Delta z}{\Delta t} \quad (8)$$

$$a_P=a_P^o+a_E+a_W+a_N+a_S+a_T+a_B \quad (9).$$

For each control volume the associated set of algebraic equations is to be solved. Boundary conditions are defined for all body surfaces according to the conditions in the experimental part.

3 DESCRIPTIONS OF MODELS AND MEASUREMENT PROCEDURE

Investigations were carried out for two models: the first one simulated the existence of air in the steel plate and the second defects due to corrosion.

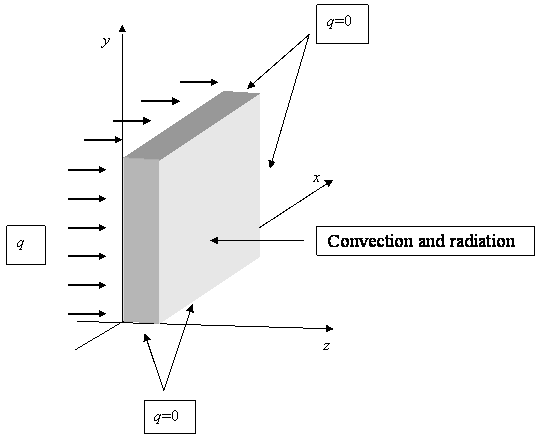

$y = 0$, $y = h$	adiabatic boundary condition
$x = 0$, $x = b$	adiabatic boundary condition
$z = 0$	thermal simulation of the object in a defined time interval, free convection and heat radiation after heating
$z = \delta$	free convection and heat radiation, ambient temperature ϑ_o, temperature of the object in ambient ϑ_{ob}.

Fig. 1. *Boundary conditions*

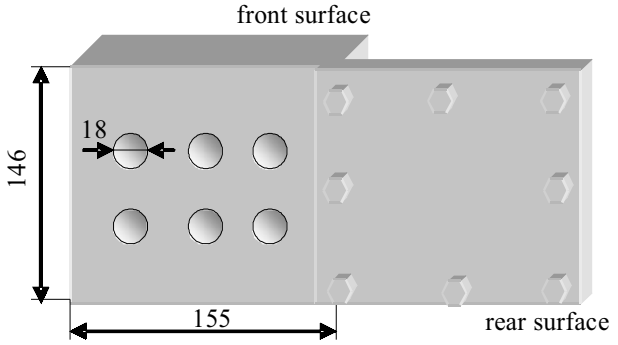

Fig. 2. *Model #1 geometry*

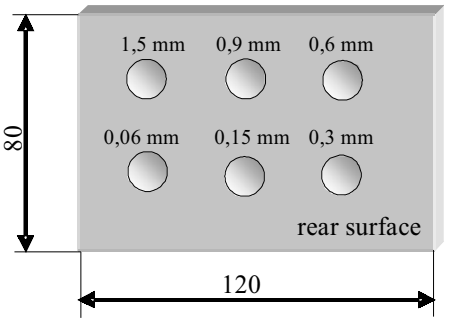

Fig. 3. *Model #2 geometry*

3.1 Model #1

Figure 2 represents the model geometry. The model consists of two 146 × 155 mm steel plates. In the base plate, which is 19 mm thick, cylindrical recesses 18 mm in diameter are milled, representing defects at various depths from the inspected surface. The 5 mm thick cover plate is tightly screwed to the base plate. The height of the cylinders milled into the base plate is in the range from 14 mm to 18 mm, so their distance from the inspection surface is between 5 mm and 1 mm [3].

The properties of the used steel are as follows: thermal conductivity $\lambda = 35$ W/(mK), thermal diffusivity $a = 9.96 \cdot 10^{-6}$ m^2/s. The model is mounted into a wooden frame that is filled with thermal insulation, so that at the lateral sides of the model an adiabatic boundary condition may be assumed. The thermal simulation of the model is performed using a 500 W spotlight. The heat radiation of the spotlight is directed through an aluminium sheet channel to the cover plate surface, and the temperature distribution is recorded on the opposite side of the model. For the numerical simulation a uniform thermal stimulation of the object is assumed. The temperature distribution at the object surface was measured using the IR AGA 680 STANDARD camera.

3.2. Model #2

The model for the simulation of the corrosion defects was a steel plate with dimensions 120 x 80 × 3 mm, as shown in Figure 3. The corroded areas are represented by six cylindrical recesses of 10 mm in diameter. The depth of each defect represents a particular loss of material caused by corrosion. For the numerical part of the investigation, corrosion is defined as a reduction of the material thickness, neglecting any changes in thermal properties of the material that may occur due to chemical reactions involved in the corrosion process.

The smooth front surface of the model was stimulated at the beginning of the simulation with a heat flux having a total energy of 78 J in a 5 ms time interval. The model was made of steel with known thermal properties, i.e., thermal conductivity $\lambda = 32$ W/(mK), thermal diffusivity $a = 1.65 \cdot 10^{-5}$ m^2/s. It is assumed that the thermal stimulation is uniform along the sample surface.

4 RESULTS OF THE NUMERICAL SIMULATION AND COMPARISON MEASUREMENTS

The problem was solved numerically by using the control-volume method. For solving the system of algebraic equations, the Gauss-Seidel procedure was used. The total number of control volumes was 15 960 for model #1, and 29 120 for model #2. The control-volume mesh was adapted to the observed problem. The mesh was condensed in the areas where steeper temperature gradients were expected.

The time step was also adapted to the stability and accuracy requirements of the discretized equation, so $\Delta t = 0.04$ s was adopted for model #1 and $\Delta t = 0.001$ s for model #2. The initial condition of the simulation assumed a model of uniform temperature.

4.1 Comparison of results

Model #1

The investigations carried out on model #1 were aimed to show the ability of the thermographic method to be used in the detection of defects under the surface in objects made of materials with a good

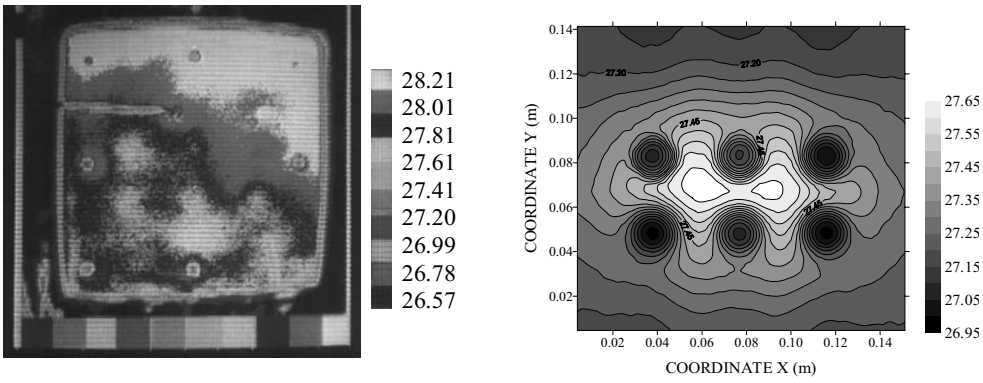

a) b)

Fig. 4. *Temperature distribution at the smooth surface of model #1 after 120 s: a) experimentally recorded thermogram, b) result obtained by numerical simulation*

thermal conductivity, and to show the possibility of detecting the defect geometry, i.e., its dimensions and position (depth) in the object. It was shown that the detection of defect shape was better in short observation times, more shallow defects are easier to recognize, the maximum instantaneous contrast is directly connected with the distance of the defect from the observed surface, regardless of its dimensions.

Figure 4 shows a comparison of the experimental results and the numerical simulation. A relatively fair agreement between the results can be seen. In the thermogram on the left, in the upper right-hand corner there is an area of higher temperature, which can be explained by experimental noise rather than a measurement error. The contrast values are rather small, so in the recorded thermogram the deeper defects are barely noticeable.

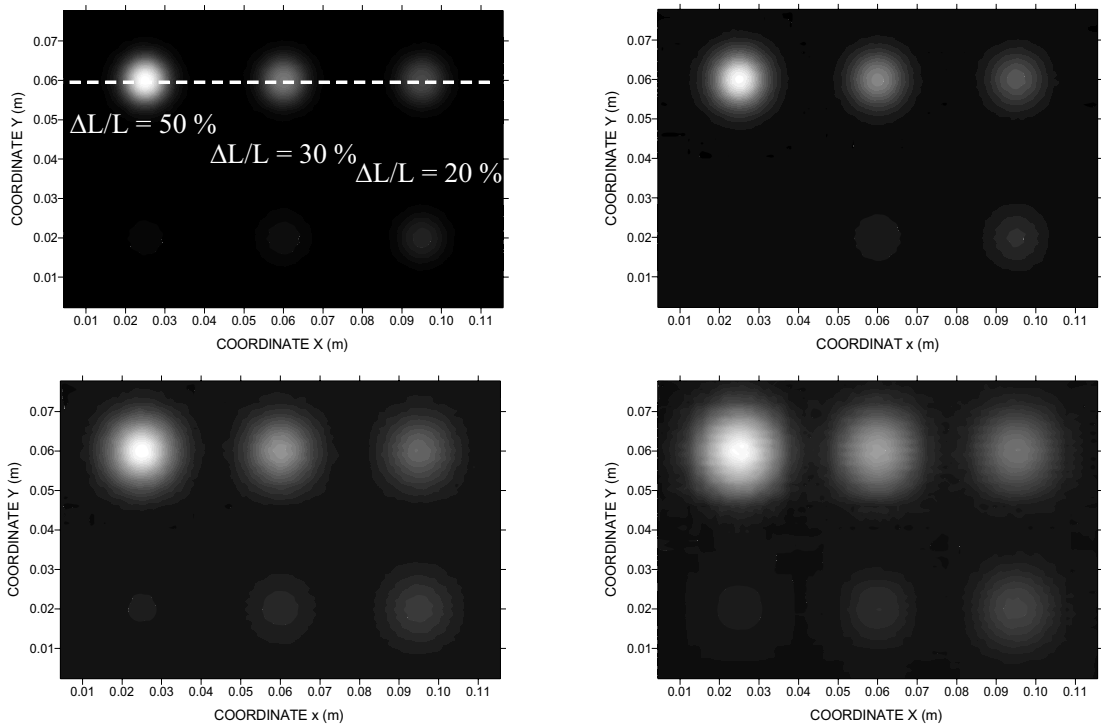

Fig. 5. *Numerically obtained temperature distributions on the front plate surface at 280 ms, 400 ms, 600 ms and 1000 ms time increments*

Model #2

The investigations carried out on model #2 were aimed to show the possibility of corrosion detection with thin metal plates. This paper presents the results of the numerical simulation carried out by the authors, and their comparison with the data obtained experimentally by Marinetti, Bison and Grinzato [4].

Temperature distributions at the plate surface for different time increments are shown in Figure 5.

A comparison of numerical and experimental results, as described in the literature [4], using the temperature distribution along the white dotted line in the thermogram for the time increment 280 ms in Figure 5, displays a very good agreement.

The corrosion degree estimation can be performed by using one of the inverse methods. The simplest algorithm relates the relative material loss and the instantaneous contrast in the following equation:

$$\frac{\Delta L}{L} = \frac{C(x,y,\tau_\infty)}{1+C(x,y,\tau_\infty)} \qquad (10).$$

The time interval during which the temperature response at the material surface is observed is most frequently expressed non-dimensionally, i.e., using the Fourier number:

$$Fo = \frac{a \cdot \tau}{L^2} \qquad (11),$$

where a is the thermal diffusivity of the material, (m^2/s), τ is the time interval, (s), and L is the thickness of the plate, (m).

For large defects the heat transport can be reduced to a one-dimensional problem. The optimal inspection time is in the range Fo ≈ 0.6 to 2.0, and Equation (10) is recommended. The characterization of smaller defects of complex shape is recommended in the interval Fo ≈ 0.3 to 0.6 [5].

Due to the three-dimensional heat diffusion the defect detection is more difficult, so it is recommended to use the temperature derivative by time according to the following equation:

$$M(x,y) = \frac{T(x,y,\tau_1) - T(x,y,\tau_2)}{\tau_1 - \tau_2} \qquad (12).$$

In every case the shape of the corroded area is more precisely indicated in a shorter inspection time interval, but with a somewhat lower amplitude [5].

Figure 7 displays the temporal distribution of values according to Equation (10). In contrast to the data from [4], where the analysis was done for Fo = 0.68, the numerical simulation shows that the best results are obtained by inspection during the time of peak temperature contrast [3]. For all defects this was in the range Fo ≈ 0.21 to 0.32.

It is also important to select a reference point T_{nd} sufficiently far from the defect itself [6].

Table 1

Effective corrosion $\Delta L/L$	Estimation time Fo	Estimation of corrosion $\Delta L/L$	Error %
0.02	0.21	0.0199	-0.5
0.05	0.242	0.0466	-6.8
0.1	0.264	0.0902	-9.8
0.2	0.292	0.175	-12.5
0.3	0.31	0.264	-12.0
0.5	0.32	0.455	-9.0

The estimation of corrosion for particular defects is shown in Table 1.

The optimum time interval to estimate the defect contours (time interval during which the defect contours in the thermogram may be most accurately identified) is also the time interval for achieving the

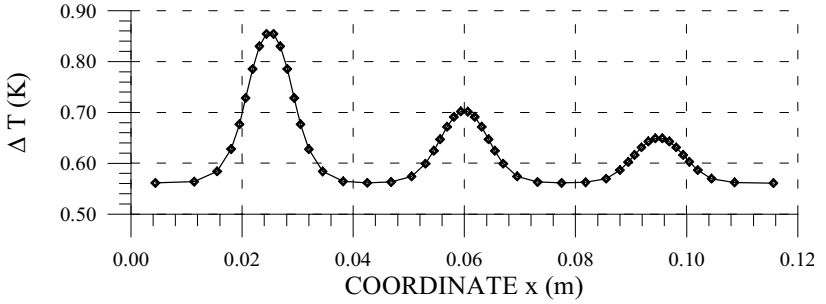

Fig. 6. *Temperature distribution on the dotted white line from Fig. 5 at time increment 0.28 s - numerical result*

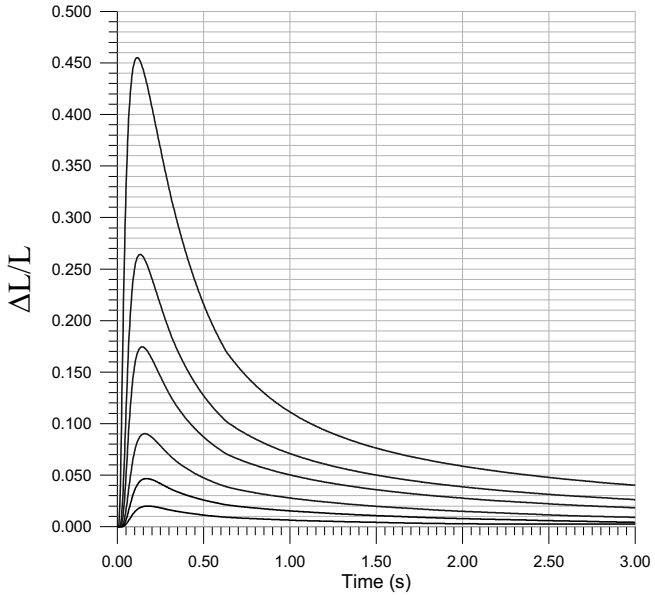

Fig. 7. *Time dependent distributions according to Equation (10)*

peak ΔT, where the reading of the diameter of each particular defect is done at half of the amplitude. Figure 8 displays the line temperature distributions along the defects in the time instant Fo = 0.28 (τ = 0.15 s).

The effective diameter of all the defects was 10 mm. The measured defect diameters are given in Table 2.

According to the literature data, material loss defects above some 20 % may be detected by thermography. The temperature time derivative according to equation (11) increases partially the defect visibility. In Figure 9, where the three-dimensional surface temperature distribution in the time instant

Table 2

Effective corrosion $\Delta L/L$	0.02	0.05	0.1	0.2	0.3	0.5
Measured defect diameter mm	10.16	10.16	9.83	9.83	9.83	9.5

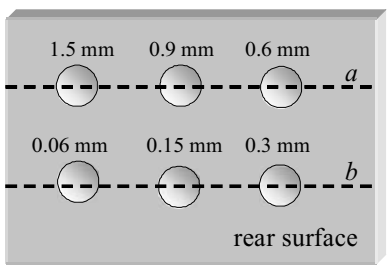

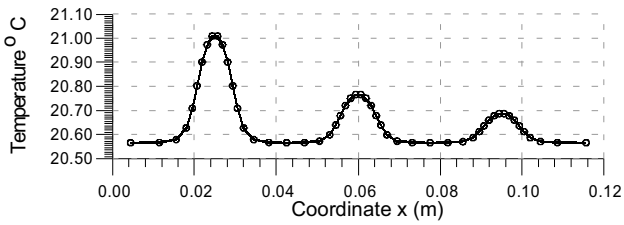

a)

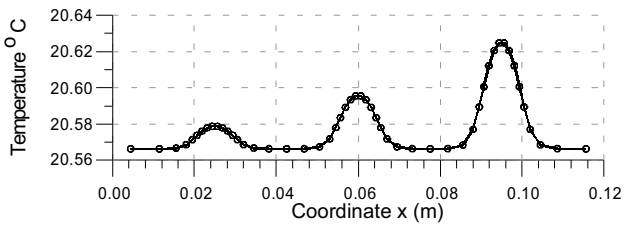

b)

Fig. 8. *a) Line temperature distribution for cross-section a; b) Line temperature distribution for cross-section b*

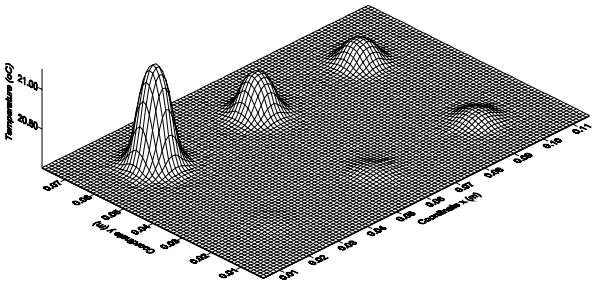

Fig. 9. *Temperature distribution for the time instant 0.1 s*

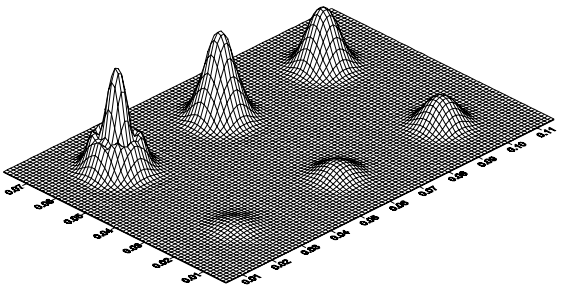

Fig. 10. *Temperature time derivative (0.05 to 0.1 s)*

0.1 s is shown, the smallest defect is not visible. On the other hand, the time derivative of temperature for $\tau_1 = 0.05$ s and τ_2 0.1 s in Figure 10 displays all the defects.

5 CONCLUSION

The performed investigation shows that both the thermographic and the numerical methods may be successfully employed in thermal non-destructive testing. The numerical approach enables the simulation of the influence of particular parameters, thus enabling a more universal overview of the influencing values. With the simulation of a process for a model with a defined number and distribution of defects it was established that the mutual influence of defects is very important, which may be directly concluded from the experimental part of the investigation. The numerical simulation also indicates situations when the three-dimensional diffusion cannot be neglected. It was also shown that the selection of an optimum inspection time interval is essential for a high-quality evaluation of the results. It can be concluded that a high-quality approach to thermal non-destructive testing necessarily requires a close link between experimental and numerical analyses in order to detect and determine all the relevant defect parameters.

6 REFERENCES

[1] D.P. Almond, P.M. Patel (1996) Photothermal science and technique, *Chapman & Hall*, London.
[2] S.V. Patankar (1980) Numerical heat transfer and fluid flow, *Hemisphere Publishing Corporation*, Mc Grow-Hill Book Co, Washington.
[3] I.Ilić-Boras, Š.Švaić (1997) Numerical simulation of the defect in specimen, *4th International Conference of the Slovenian Society for NDT*, Ljubljana.
[4] S.Marinetti, P.G.Bison, E.Grinzato (2002) 3D Heat flux effects in the experimental evaluation of corrosion by IR thermography, *QIRT'02, Quantitative InfraRed Thermography 6*, Dubrovnik, Croatia, 2002.
[5] E.Grinzato, V.Vavilov (1998) Corrosion evaluation by thermal image processing and 3D modelling, *Rev.Gen.Therm. Paris, France*, pp. 669-679.
[6] I. Boras, Š. Švaić (1998) Determination of the defect parameters in specimen by means of thermography and numerical methods, *Proceeding of The International Society for Optical Engineering*, San Antonio, Texas, USA, Vol. 3396, pp. 271-281.

Authors' address: Prof. Dr. Srećko Švaić
Prof. Dr. Ivanka Boras
Prof. Dr. Mladen Andrassy
Faculty of Mechanical Eng. and Naval Architecture
University of Zagreb
Ivana Lučića 5
10 000 Zagreb, Croatia
ivanka.boras@fsb.hr

Prejeto: 15.3.2006
Received:
Sprejeto: 25.10.2006
Accepted:
Odprto za diskusijo: 1 leto
Open for discussion: 1 year